Special Issue

Clinical Utility of Optical Coherence Tomography in Glaucoma

Zachary M. Dong,[1] Gadi Wollstein,[1,2] and Joel S. Schuman[1–4]

[1]University of Pittsburgh Medical Center (UPMC) Eye Center, Eye and Ear Institute, Department of Ophthalmology, University of Pittsburgh School of Medicine, Ophthalmology and Visual Science Research Center, Pittsburgh, Pennsylvania, United States
[2]Department of Bioengineering, Swanson School of Engineering, University of Pittsburgh, Pittsburgh, Pennsylvania, United States
[3]Department of Ophthalmology, New York University Langone Medical Center, New York University School of Medicine, New York, New York, United States
[4]Department of Electrical and Computer Engineering, New York University Tandon School of Engineering, Brooklyn, New York, United States

Correspondence: Joel S. Schuman, New York University Langone Medical Center, New York University School of Medicine, 462 First Avenue, NBV 5N3, New York, NY 10016, USA;
joel.schuman@nyu.edu.

Submitted: May 15, 2016
Accepted: July 8, 2016

Citation: Dong ZM, Wollstein G, Schuman JS. Clinical utility of optical coherence tomography in glaucoma. *Invest Ophthalmol Vis Sci*. 2016;57:OCT556–OCT567. DOI:10.1167/iovs.16-19933

Optical coherence tomography (OCT) has established itself as the dominant imaging modality in the management of glaucoma and retinal diseases, providing high-resolution visualization of ocular microstructures and objective quantification of tissue thickness and change. This article reviews the history of OCT imaging with a specific focus on glaucoma. We examine the clinical utility of OCT with respect to diagnosis and progression monitoring, with additional emphasis on advances in OCT technology that continue to facilitate glaucoma research and inform clinical management strategies.

Keywords: optical coherence tomography, optic nerve, glaucoma

Glaucoma is a multifactorial, progressive, degenerative optic neuropathy and is the second most common cause of blindness worldwide.[1] The disease is characterized by the death of retinal ganglion cells (RGCs) and their axons and by associated morphologic changes within the optic nerve and retinal nerve fiber layer (RNFL).[2–7] Progressive neuroretinal rim thinning and excavation of the optic nerve head (ONH) are consistent findings. Although most glaucoma types progress slowly, the disease can lead to blindness without treatment.[1,8] With treatment, glaucomatous progression can often be slowed or stopped. Accurate and early detection of glaucoma, therefore, is critical to successful management.

Various imaging modalities have increased and decreased in popularity as adjunctive technologies for the diagnosis and progression monitoring of glaucoma.[9] Optical coherence tomography (OCT) has become the technology of choice. Optical coherence tomography was first demonstrated in 1991[10] as an application of low-coherence interferometry.[11] Enabling noninvasive, high-resolution cross-sectional imaging of the retina in vivo, OCT's clinical utility for glaucoma was quickly realized.[12,13] Optical coherence tomography became commercially available in 1996 after scanning patterns with reproducible measurements were implemented by industry.[14] Optical coherence tomography has since changed the paradigm of assessment of the retina and revolutionized the management and diagnosis of glaucoma, allowing for objective and quantitative evaluation of neural structures affected by the disease, such as the macula and its individual layers, RNFL, and ONH.[15–23]

Optical coherence tomography technology has advanced since it was first applied to the eye and continues to rapidly evolve. Hardware advances in commercial systems improved resolution and increased scanning speeds. Previously available OCT instruments used a technique referred to as time-domain OCT (TD-OCT), which encoded the location reflections in the time information and related the location of the reflection to the position of the moving reference mirror, could obtain images of the fundus, discriminate glaucomatous eyes from normal, and detect change over time. However, this technology was limited by slow scan acquisition times and two-dimensional imaging.[24–33] The introduction of spectral-domain OCT (SD-OCT), which instead acquired all information within a single axial scan simultaneously through the tissue by evaluating the frequency spectrum of the interference between the stationary reference mirror and reflected light, increased reproducibility and accuracy in quantifying glaucomatous damage by further improving scan density and resolution and reducing imaging artifacts and scan acquisition time.[17,34–43] One of OCT's main strengths is its unparalleled high axial image resolutions. Previous TD-OCT B-scans had an axial resolution of approximately 10 μm, whereas the introduction of typical commercially available SD-OCT instruments improved resolution to approximately 5 μm axially with broad bandwidths at near infrared wavelengths. This greatly decreased the need for interpolation compared with TD-OCT.

Although SD-OCT significantly increased signal-to-noise ratio and decreased motion artifacts compared with TD-OCT, both are prone to image artifacts. These artifacts include speckle noise, segmentation and alignment errors, low signal quality,

software problems, and media opacities, such as reduced corneal clarity or cataracts. Fixational eye movements, such as ocular tremor, ocular drift, and microsaccades,[44] can further reduce image quality. Microsaccades can instantaneously move the fixated point an average amplitude of 30 arcminutes,[45] causing severe motion artifacts and unreliable measurements. Although SD-OCT devices still require a trained imaging technician to minimize artifacts, it is less operator dependent than TD-OCT devices.[46]

RNFL thickness was the OCT parameter most often used in glaucoma assessment and provided objective, quantitative measurements of RNFL thickness,[10] but the addition of new parameters on commercial devices, such as those from superficial and deep structures of the ONH and macula, improved clinical utility of OCT. Scanning patterns were also developed that could deliver three-dimensional (3D) data. Spectral-domain OCT has since established itself as the dominant imaging modality in the management of glaucoma, although newer technologies are on the horizon, as written below. Today, SD-OCT instruments are available commercially from multiple manufacturers.[47] Resolution, scan acquisition rates, and measurements across these devices are generally not interchangeable, but their ability to detect glaucoma is very similar.[16,48,49]

Swept-source OCT (SS-OCT), a newer generation of OCT, has recently been commercially introduced.[50] Swept-source OCT uses a longer wavelength (generally 1050 nm) compared with SD-OCT (840 nm).[51] Swept-source OCT can evaluate RNFL and macular thickness, but can also more clearly image deeper ocular structures such as the choroid and lamina cribrosa (LC) in patients.[51–54] With SD-OCT, it is challenging to image deep structures due to relatively poor wavelength penetrance and decreasing sensitivity and resolution with increasing depth.[55] Repeatable and automated methods of quantification and visualization of LC, however, have been developed in SD-OCT augmented with techniques for correcting for optical aberrations in the eye[56] or with enhanced depth imaging,[57–60] which simply involves moving the SD-OCT device closer to the eye, allowing use of the image on the side of the zero delay opposite from the one utilized conventionally, with consequent improved signal from deeper structures rather than more anterior ones.[61–63] Swept-source OCT is able to scan at higher speeds and can acquire high-quality wide-angle scans that contain a large area of the posterior pole, including both the optic disc and macula.

The advent of SS-OCT systems also considerably improved the visualization of the anterior chamber (AC) structures, permitting objective quantitative analysis of the AC angle and facilitating comprehensive 3D assessment of the angle. Anterior segment OCT has improved with faster scanning speeds and newer algorithms for measurement of AC parameters and is generally more sensitive in detecting angle-closure when compared to gonioscopy.[64] Swept-source OCT affords high repeatability in terms of anterior chamber angle width measurements, such as angle opening distance, trabecular iris space area, and trabecular iris angle[65] and is able to capture extremely high resolution images of the AC. A consistent measurement of iris volume and the area of peripheral anterior synechiae is now possible with SS-OCT, whereas prior generations of OCT could not reliably assess these AC parameters.[66–69] Optical coherence tomography for evaluation of the anterior segment continues to evolve and will likely have an important role in the diagnosis and management of glaucoma patients.[70]

The application of OCT has also recently been extended to angiography and blood flow measurement. Techniques to perform OCT angiography recently became commercially available,[71] and ongoing studies are exploring the link between blood flow and glaucoma. Optical coherence tomography angiography offers a repeatable,[72] high-resolution, 3D quantitative evaluation of retinal vascular abnormalities in vivo and is a promising alternative to dye-based angiography, avoiding the dye injection-related complications. Reduced retinal perfusion in the ONH and peripapillary retina has been observed in glaucomatous eyes.[72–75] Whether decreased ocular blood flow in the ONH is the cause or the result of glaucoma progression remains unresolved.[71]

These methods are also not without limitations. The cross-sectional angiograms of OCT angiography devices, for example, often show projection artifacts[76,77] due to fluctuating shadows from the blood in the inner retinal vessels. Although these artifacts may be accounted for and removed, shadows from the choriocapillaris often obscure visualization of deeper choroidal vessels. Furthermore, OCT angiography may be unable to detect extremely slow blood flow, as is present in some pathologic conditions. Doppler OCT, although able to detect to motion parallel to the OCT beam, has a limited ability to visualize motion predominantly perpendicular to the probe, such as is the case in retinal and choroidal circulations. Although hemodynamic parameters may be useful in diagnosis[78] and management of glaucoma, its true clinical utility remains to be determined.

Diagnosis of Glaucoma

Glaucomatous structural damage often precedes vision loss.[24,79–84] Although diagnosis of moderate to severe cases of glaucoma is relatively straightforward, with diagnoses confirmed based on the presence of typical visual field (VF) defects on standard automated perimetry (SAP) and corresponding signs of glaucomatous ONH damage, the disease typically remains asymptomatic in the early stages. Standard automated perimetry has been widely used for diagnosis, staging, and monitoring of glaucoma, but is only likely to detect functional deficits after at least 20%–40% of RGCs have been lost.[3,24,78–80] Furthermore, visual field testing is often variable, and diagnosis may require repeated testing.[85,86] Identification of early glaucomatous structural damage, such as structural remodeling of the ONH and inner retinal layers, is essential for early diagnosis, management, and prevention of vision loss.[87–89]

Clinical assessment using multiple parameters, including peripapillary RNFL, ONH, and macular parameters, has proven useful, not only for management and diagnosing glaucoma at various levels of severity, but for evaluating risk in glaucoma suspects.[90] Although the use of multiple parameters could increase false-positive results, structural damage may be present in one parameter and not the other, and thus it is helpful to have information from the macula, ONH, and RNFL in glaucoma diagnosis.[78,84]

Current SD-OCT RNFL thickness parameters alone, however, have good diagnostic accuracy and help clinicians in determining severity stages and differentiating normal from glaucomatous eyes in the early stages.[40,48] Retinal nerve fiber layer parameters most extensively researched include: global average circumpapillary RNFL thickness (average of thickness measurements in the circumpapillary circle centered on the ONH), thickness deviation map, and thickness parameters measured by quadrants or clock-hour sectors. In general, average circumpapillary RNFL thickness and inferior sector RNFL thicknesses are the OCT parameters with the best diagnostic accuracy, with superior quadrant thickness values following in terms of sensitivity.[15,20,21,23] This agrees with prior studies showing superior and inferior areas of the optic nerve most commonly affected glaucoma[91–93] (Fig. 1). The diagnostic accuracy of SS-

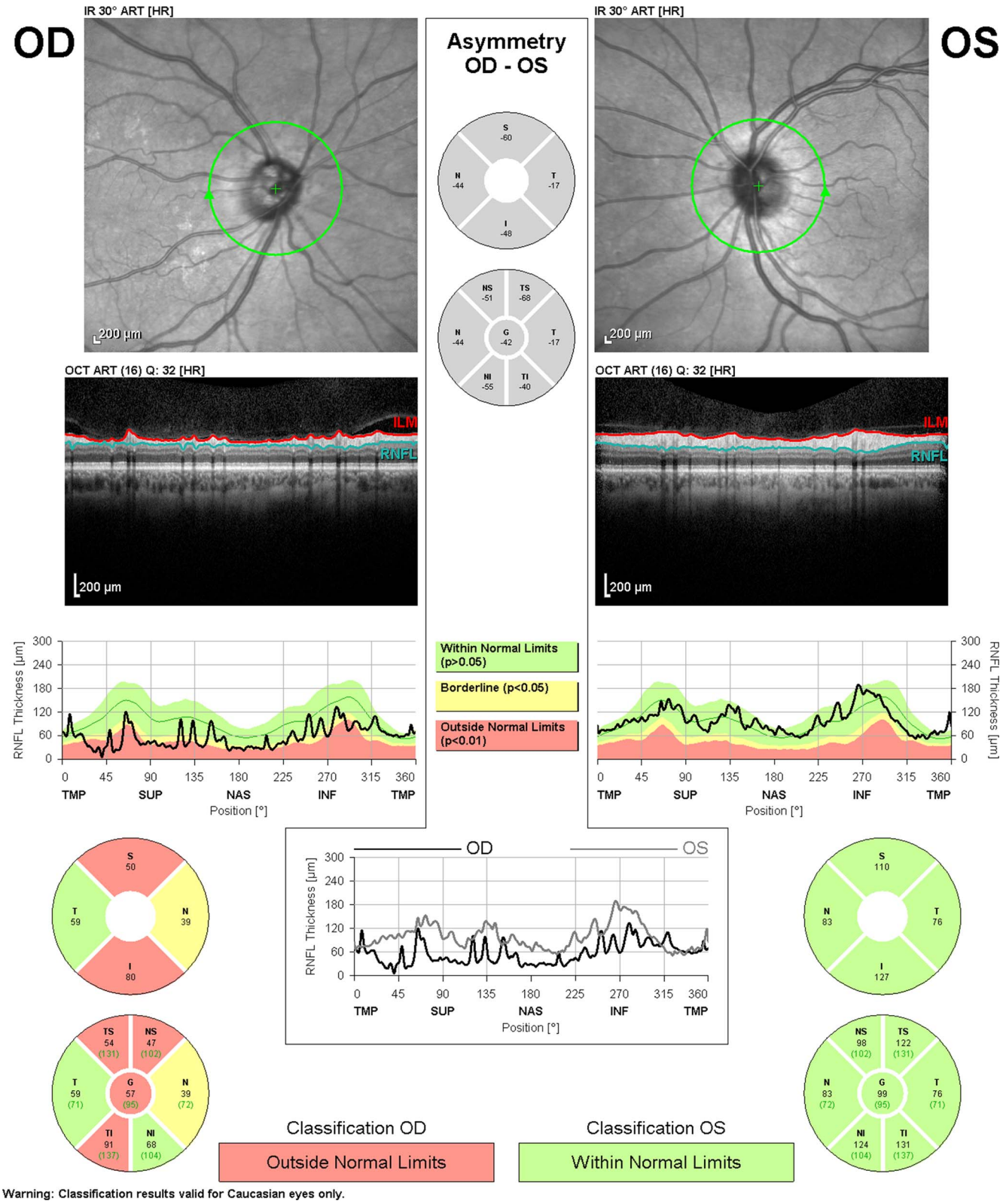

Figure 1. Retinal nerve fiber layer analysis from Spectralis-OCT (Heidelberg Engineering, Heidelberg, Germany) demonstrating glaucomatous damage. The RNFL evaluation in the right eye (OD) shows abnormalities in the superior and inferior quadrants.

OCT circumpapillary RNFL parameters are similar to those of SD-OCT.[94] For detection of glaucomatous damage, the SD-OCT RNFL parameters have sensitivities ranging from 60% to 98% and specificities ranging from 80% to 95%.[15,16,18,20,21,23] Diagnostic performance decreases, however, for detection of early disease to 48% to 77% at the same specificity range for patients with minimal visual field losses.[95,96] Recent evidence shows, however, that even before the appearance of any VF defects

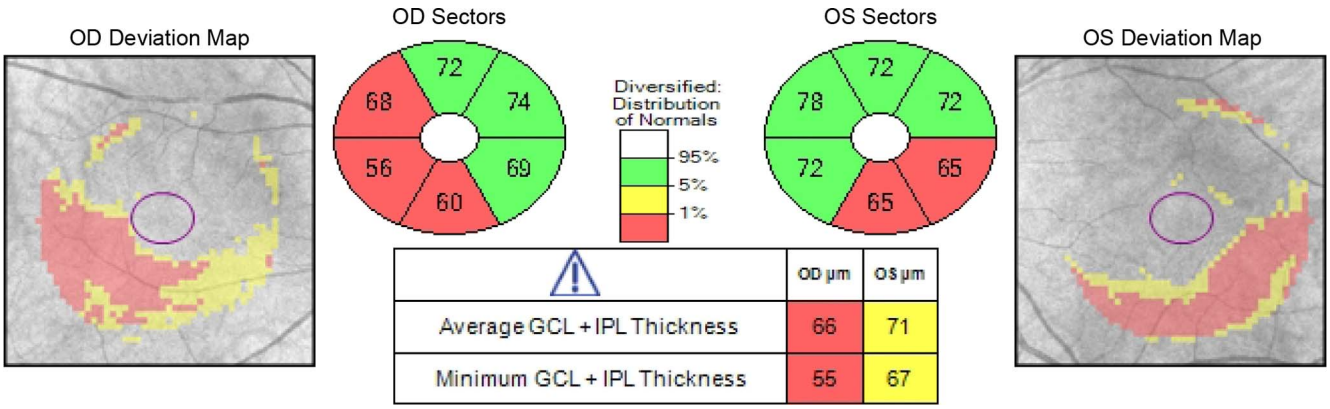

FIGURE 2. Ganglion cell analysis from Cirrus-OCT (Carl-Zeiss Meditec, Dublin, CA, USA), which includes the combination of ganglion cell and inner plexiform layers (GCIPL), shows thinning in the inferior and inferotemporal perifoveal regions of both eyes.

on SAP, RNFL average thickness parameters could detect glaucomatous damage: at 95% specificity, up to 35% of eyes had abnormal thickness values 4 years prior to detectable VF loss and 19% had abnormal values 8 years prior.[84] The reproducibility of current SD-OCT RNFL thickness parameters is excellent, with global average RNFL thickness generally being the most reproducible.[97]

Evaluation of the macular region is also important in glaucoma diagnosis; and OCT has become an attractive means for identifying glaucomatous macular damage. Glaucomatous damage of the macula is difficult to detect and generally overlooked or underestimated by clinicians when using the most common automated perimetry testing: 24-2 (6° grid) VF test.[98–105] Central structural damage can be missed with OCT reports based solely on circumpapillary RNFL.[78,106] Macular damage occurs early in the disease process and can take the form of arcuate defects, diffuse, widespread damage, and/or local damage, or some combination of these.[99,106–108] In eyes without other macular pathology, there is less variability and a lower likelihood of the presence of anomalous structural characteristics in the macula compared with the optic disc and peripapillary region.[47,109,110] Assessment of the macula may also avoid some limitations of circumpapillary measurements, such as interference from retinal and optic nerve head vasculature, peripapillary atrophy, and variable placement of the measurement circle around the disc.

Structures that thin and diminish in glaucoma comprise a large proportion of total macular thickness; these include RNFL and RGCs, but also inner plexiform layer.[111,112] The RGC layer is thickest in the perimacular region, and its thinning is likely responsible for the decreased total macular thickness observed in glaucomatous eyes. Preservation of central vision until late in the disease may suggest macular assessment is not useful for glaucoma detection. The macular RGC layer, however, is up to seven cells thick and contains more than 50% of the eye's RGCs,[113] and structural changes in the macula can thus easily precede detectable VF losses.[114] Additionally, changes in this layer are more likely be the result of pathologic change rather than normal variation,[115] and thus measurements of this layer could potentially be more sensitive than RNFL thickness parameters. Segmentation of the ganglion cell layer alone, however, remains very difficult due to low reflectivity.[116]

Advances in OCT have allowed for better quantitative evaluation of macular RGC damage and have enabled more detailed segmentation of the macular inner retinal layers and the entire macular thickness.[117–120] Although some studies show that macular RNFL (mRNFL) thickness in SD-OCT is less accurate than circumpapillary RNFL in glaucoma diagnosis or detecting preperimetric glaucoma, novel segmentation algorithms have increased the diagnostic utility of macular evaluation.[47,111,120–123] Parameters, such as mRNFL, ganglion cell layer with inner plexiform layer (CGIPL), and the ganglion cell complex (GCC), which includes mRNFL, ganglion cell layer, and inner plexiform layer,[117,118] can distinguish glaucomatous eyes from those of healthy subjects and can differentiate between early, moderate, and advanced glaucoma.[110,121,124–129] The GCC and GCIPL parameters from both SS-OCT and SD-OCT carry a diagnostic performance at least equal to that of circumpapillary RNFL parameters[130]; all three parameters, including mRNFL, now have comparable diagnostic performance in detection of preperimetric glaucoma.[110,124–126] Once VF losses are apparent, there is a significant association of VF defect patterns with GCIPL defect patterns.[114] The most commonly observed GCIPL and inner macular layer defect pattern in glaucoma subjects is thinning in the inferior perifoveal region, seen clinically as superior VF defects[100,111,131,132] (Figs. 2, 3).

Macular parameters are of increasing importance in the management of glaucoma, especially given improvements in OCT technology. Recent software updates have reduced GCC segmentation errors in patients with macular degeneration, which should allow these patients to be evaluated for glaucoma with more confidence.[133,134] Posterior pole asymmetry analysis (PPAA) combines mapping of the posterior pole retinal thickness with asymmetry analysis between eyes and between hemispheres of each eye.[135] Posterior pole asymmetry analysis, although not presently having a built-in normative database, is highly reproducible and matches circumpapillary RNFL measurements in terms of diagnostic accuracy of early glaucoma.[136–138] Spectral-domain OCT may also be superior to

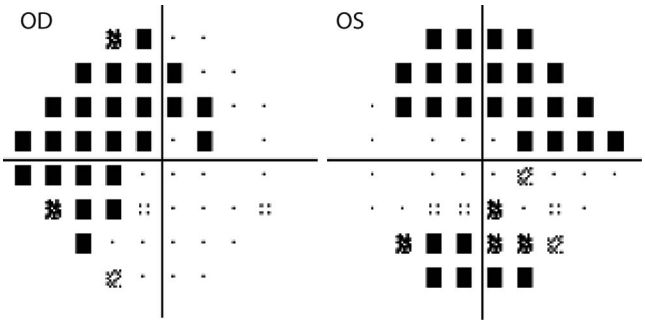

FIGURE 3. Perimetric pattern deviation maps from the same patient shown in Figure 2. Defects correspond with the locations of thinning observed in ganglion cell analysis.

SS-OCT in detecting GCIPL thinning in the outer temporal zone,[119] where the glaucomatous damage commonly occurs.[100] However, SD-OCT and SS-OCT have similar glaucoma diagnosis abilities based on macular inner layer thickness analysis.[119] Ultimately, clinical assessment of the macular region is helpful in glaucoma diagnosis and evaluation and clinicians should incorporate macular scans into clinical protocols. Patients with abnormal or borderline macular structural parameters likely require close follow-up and initiation of treatment to avoid vision loss.[139] Clinicians should not rely entirely on macular parameters, however. In addition to glaucoma, other macular diseases are also common in the aging population. These conditions may affect OCT macular thickness measurements and render them useless for the evaluation of glaucoma, including diabetic retinopathy, macular edema, macular degeneration, and epiretinal membranes.

Advances in OCT technology have also allowed for higher-resolution imaging of the ONH[140] and quantification of ONH parameters, but the clinical value of OCT ONH parameters remains controversial. Compared with previous OCT technology, SD-OCT relies less on data interpolation, and this has resulted in far better delineation of ONH structures than could be achieved with TD-OCT. Studies have found that ONH parameters have an excellent ability to discriminate between normal eyes and eyes with even mild glaucoma. Parameters such as rim area, vertical rim thickness, and vertical cup to disc ratio were found to have the greatest diagnostic ability and were as good as RNFL thickness parameters in diagnosing glaucoma.[40] In some cases, ONH parameters were found to be better at initial glaucoma detection and discriminating glaucoma and glaucoma suspect subjects from normal subjects.[141,142] However, a number of studies show ONH parameters are inferior to standard circumpapillary measurements for glaucoma detection.[122,143,144] One study, although limited by using VFs as a reference standard, found that RNFL and macular parameters were significantly better for glaucoma diagnosis than ONH parameters, especially for early-stage glaucoma.[21,143] Differences in these results are at least partially a consequence of the reference standard used to select cases and controls given that a reference standard must be employed to select cases and controls for any diagnostic accuracy study.[145] There is a greater chance, for example, that patients with clearly abnormal optic disc features will be classified as cases if the reference criteria include optic disc appearance. Retinal nerve fiber layer abnormalities are not as easily detectable by clinicians.[146,147] Similarly, those with normal appearing optic discs will be declared controls. This type of reference standard introduces a bias towards favoring accuracy of topographic ONH parameters.[145] Furthermore, differences in commercially available OCT devices could at least partially explain the differences between studies, such as differences in the acquisition speed, scanning rate, spatial resolution,[142] layer detection algorithms, and analytical software. Each of the different devices, therefore, may report different RNFL thickness values and ONH measurements. Additional reasons could also contribute to variable results, including differences in the number of subjects, differences in ethnicity, or differences in the representation of the different stages of glaucoma.[40,143] Consideration of a combination of circumpapillary and ONH parameters is likely the best approach for glaucoma detection.[29,78,141]

Given recent advances in SD-OCT technology, evaluating the ONH with OCT is useful in the diagnosis and management of glaucoma. Segmentation of the ONH was greatly improved with new software, as was implementation of referencing the fovea's position and Bruch's membrane as anatomic landmarks, which allowed for better measurement of the ONH rim and RNFL thickness.[148–150] Bruch's membrane opening minimal rim width (BMO-MRW), a relatively new anatomical parameter describing the neuroretinal rim, consists of the minimum distance between the BMO and the internal limiting membrane. Bruch's membrane opening minimal rim width has a high association with glaucomatous functional changes on SAP and, compared with previous BMO methods, has a better ability to detect early glaucoma.[142,148,151] It has an advantage over other SD-OCT methods of neuroretinal thickness measurement by considering the variable orientation of rim tissue in the ONH. Rim area, however, appears to be a more useful ONH parameter for detecting early glaucoma.[142] Ultimately, assessment of circumpapillary RNFL, macular, and ONH parameters is useful for quantifying risk, diagnosis, and management of glaucoma at different levels of severity.

Detecting Progression

Detection of disease progression remains challenging in glaucoma due to the variable and slowly progressive nature of the disease, measurement variability of SAP and of imaging devices, and the lack of a commonly acceptable reference standard.[47] Some eyes show structural changes in the ONH or RNFL before any indication of glaucomatous damage can be detected with SAP.[82] Because SD-OCT is relatively new technology, only a few reports exist using SD-OCT RNFL parameters for detecting glaucoma progression.[75,152–155] Most progression studies use TD-OCT due to the longer follow-up period.[24,32,33,156]

Assessment of multiple OCT parameters from the macula, ONH, and RNFL is important, not only in diagnosis, but to detect disease progression and longitudinal change.[78] Retinal nerve fiber layer evaluation is less sensitive than VF when tracking progression in advanced cases due to a floor effect that occurs when the residual RGC layer has nearly diminished.[156–158] Location of RNFL losses should also be considered when predicting VF progression.[32,156,159] Although average RNFL thickness may be the main parameter to consider when evaluating for structural progression in advanced glaucoma patients, RNFL thicknesses in the inferior quadrant and inferotemporal sector may be the most predictive of progression[33,156] (Fig. 4). Retinal nerve fiber layer thinning in the superior quadrant has also been associated with subsequent VF losses in TD-OCT.[160] Spectral-domain OCT instruments cannot be used interchangeably, however, especially for glaucoma progression assessment, due to variability in circumpapillary RNFL thickness calculations.[49] Interestingly, other studies found that average macular thickness is more sensitive than circumpapillary RNFL for detection of disease progression.[161] Additionally, analysis of the total retinal thickness (GCIPL, along with outer plexiform layer to RPE) may be more sensitive in detecting progression than circumpapillary RNFL.[162]

Approaches that combine structure and function improve diagnosis both in cross-sectional and longitudinal investigations[163,164] and algorithms that combine structural and functional measurements will likely improve the detection of glaucoma progression.[139,163–166] Prior studies suggest that using a combination of perimetry and circumpapillary RNFL values is the best approach when monitoring for progression, especially given that SD-OCT RNFL values have a strong relationship to functional deficits.[167–172] In TD-OCT, structural progression was associated with functional progression in preperimetric, glaucoma suspect, and glaucomatous eyes[160] and eyes with significant SAP progression have higher rates of RNFL thickness loss compared with nonprogressing eyes.[173] Clinically, it can be difficult to determine whether RNFL losses that precede SAP changes reflect true progression. Important from a clinical perspective, the 24-2 VF test, although the gold

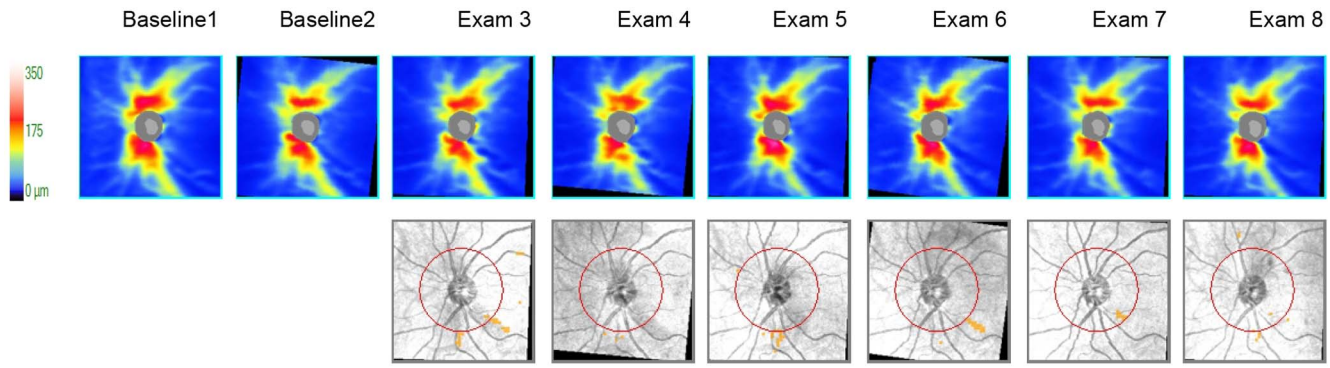

RNFL and ONH Summary Parameters

		Exam Date/Time	Serial Number	Registration Method	SS	Avg RNFL Thickness (µm)	Inf Quadrant RNFL (µm)	Sup Quadrant RNFL (µm)	Rim Area (mm^2)	Average Cup-to-Disc Ratio	Vertical Cup-to-Disc Ratio	Cup Volume (mm^3)
Baseline1:	1	12/2007	4000-1011		10/10	85	111	105	0.92	0.49	0.52	0.100
Baseline2:	2	5/2009	4000-1162	R2	8/10	82	106	105	0.90	0.49	0.49	0.092
	3	12/2011	4000-1011	R2	9/10	80	106	103	0.87	0.47	0.47	0.082
	4	7/2012	4000-1162	R2	7/10	79	104	104	0.95	0.47	0.47	0.086
	5	1/2013	4000-1011	R2	8/10	76	97	103	0.88	0.47	0.48	0.078
	6	7/2014	5000-2336	R2	8/10	79	97	104	0.94	0.49	0.50	0.092
	7	3/2015	5000-2336	R2	9/10	79	99	105	0.88	0.50	0.53	0.092
Current:	8	9/2015	5000-2336	R2	8/10	77	93	104	0.90	0.51	0.56	0.098

Registration Methods
R2 - Registration based on translation and rotation of OCT fundus
R1 - Registration based only on translation of disc center

Likely Loss
Possible Loss
Possible Increase

Compared to baseline, statistically significant loss of tissue detected. For Average RNFL, Superior RNFL, Inferior RNFL, Rim Area the values have decreased. For Cup-to-Disc Ratios and Cup Volume values have increased.

Compared to baseline, statistically significant increase detected. For Average RNFL, Superior RNFL, Inferior RNFL, Rim Area values have increased. For Cup-to-Disc Ratios and Cup Volume values have decreased.

FIGURE 4. Guided progression analysis from Cirrus-OCT (Carl-Zeiss Meditec) demonstrating early glaucomatous progression. Compared with baseline examinations from December 2007, the patient has statistically significant focal RNFL loss in the inferior quadrant in the left eye. More commonly, the corresponding RNFL thickness map to "Exam 6" may show a red wedge-shaped defect in the inferior quadrant of the ONH.

standard in SAP for glaucoma evaluation, is not an ideal strategy for detecting glaucomatous damage of the macula; the 10-2 VF will often detect damage missed with the 24-2 pattern.[98,101]

As OCT evolves, it will continue to provide more accurate detection of progression and enhance our understanding of the structural pathogenesis of glaucoma, including the role of the LC in glaucoma progression. As the presumed site of axonal injury in glaucoma,[174] the LC may play a role in neuronal death seen in glaucoma. Lamina cribrosa microstructure likely provides the mechanical support to optic nerve fibers within the deep optic disc region.[175] Quantitative measurements of LC microarchitecture, such as pore diameter, pore area, and LC

beam thickness, were found to have good reproducibility[56] in a multimodal SD-OCT with adaptive optics technology and offer the potential to serve as biomarkers for glaucoma progression. Using a prototype SS-OCT with 100,000 A-scan/s scanning speed and 5-μm axial resolution, Wang et al. demonstrated good reproducibility of LC parameters, including pore diameter SD, pore aspect ratio; beam thickness, pore area, beam thickness SD, and beam thickness to pore diameter ratio.[176] Lamina cribrosa microarchitecture changes have been observed with SS-OCT in glaucomatous eyes,[177] and LC pore shape and size also have been correlated with the severity and progression of glaucoma.[178,179] Additionally, the LC was found to be displaced both anteriorly and posteriorly in glaucomatous eyes compared with age-matched healthy eyes,[180–182] and thinner LC was associated with glaucoma progression.[183] Overall, the structural thinning and displacement of the LC likely cause LC pores to deform,[184] impeding axoplasmic flow within the optic nerve fibers and disrupting transport of factors crucial for the survival of RGCs.[185,186] This could lead to RGC apoptosis, contributing to glaucoma development and progression. In addition, there may be biological changes that occur due to deformations of the lamina in the axons or microglia that result in axonal stress or RGC impairment or death. Although the LC's role in glaucoma progression is yet to be fully determined, SS-OCT and SD-OCT have undoubtedly improved current understanding of the LC and its microarchitecture.[176]

Conclusions

Optical coherence tomography has changed the face of glaucoma assessment and research. Optical coherence tomography has impacted the ways that patients are diagnosed and followed clinically and remains a dynamic and evolving imaging modality. Optical coherence tomography technology and software algorithms are improving and newer technologies are continually under development,[187–189] increasing OCT's clinical utility. Clinicians should be aware of OCT's limitations and should be aware of possible scan artifacts. Clinical decisions should never be driven by OCT results alone, but should also be based on a complete ophthalmic examination and VF assessment.

Acknowledgments

Supported in part by National Institutes of Health National Eye Institute R01-EY013178, P30-EY008098 (Bethesda, MD, USA), The Eye and Ear Foundation (Pittsburgh, PA, USA), and Research to Prevent Blindness (New York, NY, USA).

Disclosure: **Z.M. Dong**, None; **G. Wollstein**, None; **J.S. Schuman**, Zeiss (C), P, Aerie (C), Annexon (C), Alcon (C), Opticient (C), Shire (C), Pfizer (C), SLACK/Vindico (C)

References

1. Quigley HA, Broman AT. The number of people with glaucoma worldwide in 2010 and 2020. *Br J Ophthalmol*. 2006;90:262–267.
2. Garcia-Valenzuela E, Shareef S, Walsh J, Sharma SC. Programmed cell death of retinal ganglion cells during experimental glaucoma. *Exp Eye Res*. 1995;61:33–44.
3. Quigley HA, Dunkelberger GR, Green WR. Retinal ganglion cell atrophy correlated with automated perimetry in human eyes with glaucoma. *Am J Ophthalmol*. 1989;107:453–464.
4. Quigley HA, Nickells RW, Kerrigan LA, Pease ME, Thibault DJ, Zack DJ. Retinal ganglion cell death in experimental glaucoma and after axotomy occurs by apoptosis. *Invest Ophthalmol Vis Sci*. 1995;36:774–786.
5. Sommer A, Miller NR, Pollack I, Maumenee AE, George T. The nerve fiber layer in the diagnosis of glaucoma. *Arch Ophthalmol*. 1977;95:2149–2156.
6. Weinreb RN, Aung T, Medeiros FA. The pathophysiology and treatment of glaucoma: a review. *JAMA*. 2014;311:1901–1911.
7. Weinreb RN, Khaw PT. Primary open-angle glaucoma. *Lancet*. 2004;363:1711–1720.
8. Foster PJ, Buhrmann R, Quigley HA, Johnson GJ. The definition and classification of glaucoma in prevalence surveys. *Br J Ophthalmol*. 2002;86:238–242.
9. Girach A, Sergott RC. *Optical Coherence Tomography*. New York: Springer; 2016.
10. Huang D, Swanson EA, Lin CP, et al. Optical coherence tomography. *Science*. 1991;254:1178–1181.
11. Fercher AF, Mengedoht K, Werner W. Eye-length measurement by interferometry with partially coherent light. *Opt Lett*. 1988;13:186–188.
12. Schuman JS, Hee MR, Arya AV, et al. Optical coherence tomography: a new tool for glaucoma diagnosis. *Curr Opin Ophthalmol*. 1995;6:89–95.
13. Puliafito CA, Hee MR, Lin CP, et al. Imaging of macular diseases with optical coherence tomography. *Ophthalmology*. 1995;102:217–229.
14. Schuman JS, Pedut-Kloizman T, Hertzmark E, et al. Reproducibility of nerve fiber layer thickness measurements using optical coherence tomography. *Ophthalmology*. 1996;103:1889–1898.
15. Kim JS, Ishikawa H, Gabriele ML, et al. Retinal nerve fiber layer thickness measurement comparability between time domain optical coherence tomography (OCT) and spectral domain OCT. *Invest Ophthalmol Vis Sci*. 2010;51:896–902.
16. Leite MT, Rao HL, Zangwill LM, Weinreb RN, Medeiros FA. Comparison of the diagnostic accuracies of the Spectralis, Cirrus, and RTVue optical coherence tomography devices in glaucoma. *Ophthalmology*. 2011;118:1334–1339.
17. Leung CK, Cheung CY, Weinreb RN, et al. Retinal nerve fiber layer imaging with spectral-domain optical coherence tomography: a variability and diagnostic performance study. *Ophthalmology*. 2009;116:1257–1263.
18. Leung CK, Lam S, Weinreb RN, et al. Retinal nerve fiber layer imaging with spectral-domain optical coherence tomography: analysis of the retinal nerve fiber layer map for glaucoma detection. *Ophthalmology*. 2010;117:1684–1691.
19. Medeiros FA, Zangwill LM, Bowd C, Weinreb RN. Comparison of the GDx VCC scanning laser polarimeter, HRT II confocal scanning laser ophthalmoscope, and stratus OCT optical coherence tomograph for the detection of glaucoma. *Arch Ophthalmol*. 2004;122:827–837.
20. Park SB, Sung KR, Kang SY, Kim KR, Kook MS. Comparison of glaucoma diagnostic Capabilities of Cirrus HD and Stratus optical coherence tomography. *Arch Ophthalmol*. 2009;127:1603–1609.
21. Rao HL, Zangwill LM, Weinreb RN, Sample PA, Alencar LM, Medeiros FA. Comparison of different spectral domain optical coherence tomography scanning areas for glaucoma diagnosis. *Ophthalmology*. 2010;117:1692–1699.
22. Sehi M, Grewal DS, Sheets CW, Greenfield DS. Diagnostic ability of Fourier-domain vs time-domain optical coherence tomography for glaucoma detection. *Am J Ophthalmol*. 2009;148:597–605.
23. Wang X, Li S, Fu J, et al. Comparative study of retinal nerve fibre layer measurement by RTVue OCT and GDx VCC. *Br J Ophthalmol*. 2011;95:509–513.

24. Wollstein G, Schuman JS, Price LL, et al. Optical coherence tomography longitudinal evaluation of retinal nerve fiber layer thickness in glaucoma. *Arch Ophthalmol*. 2005;123:464–470.
25. Medeiros FA, Zangwill LM, Bowd C, Vessani RM, Susanna R, Jr, Weinreb RN. Evaluation of retinal nerve fiber layer, optic nerve head, and macular thickness measurements for glaucoma detection using optical coherence tomography. *Am J Ophthalmol*. 2005;139:44–55.
26. Manassakorn A, Nouri-Mahdavi K, Caprioli J. Comparison of retinal nerve fiber layer thickness and optic disk algorithms with optical coherence tomography to detect glaucoma. *Am J Ophthalmol*. 2006;141:105–115.
27. Hougaard JL, Heijl A, Bengtsson B. Glaucoma detection by Stratus OCT. *J Glaucoma*. 2007;16:302–306.
28. Hougaard JL, Heijl A, Bengtsson B. Glaucoma detection using different Stratus optical coherence tomography protocols. *Acta Ophthalmol Scand*. 2007;85:251–256.
29. Naithani P, Sihota R, Sony P, et al. Evaluation of optical coherence tomography and heidelberg retinal tomography parameters in detecting early and moderate glaucoma. *Invest Ophthalmol Vis Sci*. 2007;48:3138–3145.
30. Parikh RS, Parikh S, Sekhar GC, et al. Diagnostic capability of optical coherence tomography (Stratus OCT 3) in early glaucoma. *Ophthalmology*. 2007;114:2238–2243.
31. Nouri-Mahdavi K, Nikkhou K, Hoffman DC, Law SK, Caprioli J. Detection of early glaucoma with optical coherence tomography (StratusOCT). *J Glaucoma*. 2008;17:183–188.
32. Lee EJ, Kim TW, Park KH, Seong M, Kim H, Kim DM. Ability of Stratus OCT to detect progressive retinal nerve fiber layer atrophy in glaucoma. *Invest Ophthalmol Vis Sci*. 2009;50:662–668.
33. Medeiros FA, Zangwill LM, Alencar LM, et al. Detection of glaucoma progression with stratus OCT retinal nerve fiber layer, optic nerve head, and macular thickness measurements. *Invest Ophthalmol Vis Sci*. 2009;50:5741–5748.
34. Ortega Jde L, Kakati B, Girkin CA. Artifacts on the optic nerve head analysis of the optical coherence tomography in glaucomatous and nonglaucomatous eyes. *J Glaucoma*. 2009;18:186–191.
35. Iliev ME, Meyenberg A, Garweg JG. Morphometric assessment of normal, suspect and glaucomatous optic discs with Stratus OCT and HRT II. *Eye (Lond)*. 2006;20:1288–1299.
36. Knight OJ, Chang RT, Feuer WJ, Budenz DL. Comparison of retinal nerve fiber layer measurements using time domain and spectral domain optical coherent tomography. *Ophthalmology*. 2009;116:1271–1277.
37. Johnson DE, El-Defrawy SR, Almeida DR, Campbell RJ. Comparison of retinal nerve fibre layer measurements from time domain and spectral domain optical coherence tomography systems. *Can J Ophthalmol*. 2009;44:562–566.
38. Gonzalez-Garcia AO, Vizzeri G, Bowd C, Medeiros FA, Zangwill LM, Weinreb RN. Reproducibility of RTVue retinal nerve fiber layer thickness and optic disc measurements and agreement with Stratus optical coherence tomography measurements. *Am J Ophthalmol*. 2009;147:1067–1074.
39. Kim JS, Ishikawa H, Sung KR, et al. Retinal nerve fibre layer thickness measurement reproducibility improved with spectral domain optical coherence tomography. *Br J Ophthalmol*. 2009;93:1057–1063.
40. Mwanza JC, Oakley JD, Budenz DL, Anderson DR. Cirrus Optical Coherence Tomography Normative Database Study G. Ability of cirrus HD-OCT optic nerve head parameters to discriminate normal from glaucomatous eyes. *Ophthalmology*. 2011;118:241–248.
41. Sung KR, Kim JS, Wollstein G, Folio L, Kook MS, Schuman JS. Imaging of the retinal nerve fibre layer with spectral domain optical coherence tomography for glaucoma diagnosis. *Br J Ophthalmol*. 2011;95:909–914.
42. Leung CK, Liu S, Weinreb RN, et al. Evaluation of retinal nerve fiber layer progression in glaucoma a prospective analysis with neuroretinal rim and visual field progression. *Ophthalmology*. 2011;118:1551–1557.
43. Schuman JS. Spectral domain optical coherence tomography for glaucoma (an AOS thesis). *Trans Am Ophthalmol Soc*. 2008;106:426–458.
44. Martinez-Conde S, Macknik SL, Hubel DH. The role of fixational eye movements in visual perception. *Nat Rev Neurosci*. 2004;5:229–240.
45. Masquelier T, Portelli G, Kornprobst P. Microsaccades enable efficient synchrony-based coding in the retina: a simulation study. *Sci Rep*. 2016;6:24086.
46. Hardin JS, Taibbi G, Nelson SC, Chao D, Vizzeri G. Factors affecting Cirrus-HD OCT optic disc scan quality: a review with case examples. *J Ophthalmol*. 2015;2015:746150.
47. Grewal DS, Tanna AP. Diagnosis of glaucoma and detection of glaucoma progression using spectral domain optical coherence tomography. *Curr Opin Ophthalmol*. 2013;24:150–161.
48. Akashi A, Kanamori A, Nakamura M, Fujihara M, Yamada Y, Negi A. Comparative assessment for the ability of Cirrus, RTVue, and 3D-OCT to diagnose glaucoma. *Invest Ophthalmol Vis Sci*. 2013;54:4478–4484.
49. Pierro L, Gagliardi M, Iuliano L, Ambrosi A, Bandello F. Retinal nerve fiber layer thickness reproducibility using seven different OCT instruments. *Invest Ophthalmol Vis Sci*. 2012;53:5912–5920.
50. Chinn SR, Swanson EA, Fujimoto JG. Optical coherence tomography using a frequency-tunable optical source. *Opt Lett*. 1997;22:340–342.
51. Mansouri K, Nuyen B, N Weinreb R. Improved visualization of deep ocular structures in glaucoma using high penetration optical coherence tomography. *Expert Rev Med Devices*. 2013;10:621–628.
52. Mansouri K, Medeiros FA, Marchase N, Tatham AJ, Auerbach D, Weinreb RN. Assessment of choroidal thickness and volume during the water drinking test by swept-source optical coherence tomography. *Ophthalmology*. 2013;120:2508–2516.
53. Takayama K, Hangai M, Kimura Y, et al. Three-dimensional imaging of lamina cribrosa defects in glaucoma using swept-source optical coherence tomography. *Invest Ophthalmol Vis Sci*. 2013;54:4798–4807.
54. Park HY, Shin HY, Park CK. Imaging the posterior segment of the eye using swept-source optical coherence tomography in myopic glaucoma eyes: comparison with enhanced-depth imaging. *Am J Ophthalmol*. 2014;157:550–557.
55. Miki A, Ikuno Y, Jo Y, Nishida K. Comparison of enhanced depth imaging and high-penetration optical coherence tomography for imaging deep optic nerve head and parapapillary structures. *Clin Ophthalmol*. 2013;7:1995–2001.
56. Nadler Z, Wang B, Wollstein G, et al. Repeatability of in vivo 3D lamina cribrosa microarchitecture using adaptive optics spectral domain optical coherence tomography. *Biomed Opt Express*. 2014;5:1114–1123.
57. Park HY, Jeon SH, Park CK. Enhanced depth imaging detects lamina cribrosa thickness differences in normal tension glaucoma and primary open-angle glaucoma. *Ophthalmology*. 2012;119:10–20.
58. Park SC, De Moraes CG, Teng CC, Tello C, Liebmann JM, Ritch R. Enhanced depth imaging optical coherence tomography of deep optic nerve complex structures in glaucoma. *Ophthalmology*. 2012;119:3–9.
59. Park HY, Lee NY, Shin HY, Park CK. Analysis of macular and peripapillary choroidal thickness in glaucoma patients by

Investigative Ophthalmology & Visual Science

enhanced depth imaging optical coherence tomography. *J Glaucoma*. 2014;23:225–231.

60. Lee EJ, Kim TW, Weinreb RN, et al. Three-dimensional evaluation of the lamina cribrosa using spectral-domain optical coherence tomography in glaucoma. *Invest Ophthalmol Vis Sci*. 2012;53:198–204.
61. Fujiwara T, Imamura Y, Margolis R, Slakter JS, Spaide RF. Enhanced depth imaging optical coherence tomography of the choroid in highly myopic eyes. *Am J Ophthalmol*. 2009; 148:445–450.
62. Fujiwara A, Shiragami C, Shirakata Y, Manabe S, Izumibata S, Shiraga F. Enhanced depth imaging spectral-domain optical coherence tomography of subfoveal choroidal thickness in normal Japanese eyes. *Jpn J Ophthalmol*. 2012;56:230–235.
63. Margolis R, Spaide RF. A pilot study of enhanced depth imaging optical coherence tomography of the choroid in normal eyes. *Am J Ophthalmol*. 2009;147(5):811–815.
64. Nolan WP, See JL, Chew PT, et al. Detection of primary angle closure using anterior segment optical coherence tomography in Asian eyes. *Ophthalmology*. 2007;114:33–39.
65. Liu S, Yu M, Ye C, Lam DS, Leung CK. Anterior chamber angle imaging with swept-source optical coherence tomography: an investigation on variability of angle measurement. *Invest Ophthalmol Vis Sci*. 2011;52:8598–8603.
66. Mak H, Xu G, Leung CK. Imaging the iris with swept-source optical coherence tomography: relationship between iris volume and primary angle closure. *Ophthalmology*. 2013; 120:2517–2524.
67. Tun TA, Baskaran M, Perera SA, et al. Sectoral variations of iridocorneal angle width and iris volume in Chinese Singaporeans: a swept-source optical coherence tomography study. *Graefes Arch Clin Exp Ophthalmol*. 2014;252:1127–1132.
68. Invernizzi A, Giardini P, Cigada M, Viola F, Staurenghi G. Three-dimensional morphometric analysis of the iris by swept-source anterior segment optical coherence tomography in a Caucasian population. *Invest Ophthalmol Vis Sci*. 2015;56:4796–4801.
69. Lai I, Mak H, Lai G, Yu M, Lam DS, Leung CK. Anterior chamber angle imaging with swept-source optical coherence tomography: measuring peripheral anterior synechia in glaucoma. *Ophthalmology*. 2013;120:1144–1149.
70. Maslin JS, Barkana Y, Dorairaj SK. Anterior segment imaging in glaucoma: an updated review. *Indian J Ophthalmol*. 2015; 63:630–640.
71. Nakazawa T. Ocular blood flow and influencing factors for glaucoma. *Asia Pac J Ophthalmol (Phila)*. 2016;5:38–44.
72. Jia Y, Wei E, Wang X, et al. Optical coherence tomography angiography of optic disc perfusion in glaucoma. *Ophthalmology*. 2014;121:1322–1332.
73. Wang X, Jiang C, Ko T, et al. Correlation between optic disc perfusion and glaucomatous severity in patients with open-angle glaucoma: an optical coherence tomography angiography study. *Graefes Arch Clin Exp Ophthalmol*. 2015;253: 1557–1564.
74. Jia Y, Tan O, Tokayer J, et al. Split-spectrum amplitude-decorrelation angiography with optical coherence tomography. *Opt Express*. 2012;20:4710–4725.
75. Liu L, Jia Y, Takusagawa HL, et al. Optical coherence tomography angiography of the peripapillary retina in glaucoma. *JAMA Ophthalmol*. 2015;133:1045–1052.
76. Yu L, Chen Z. Doppler variance imaging for three-dimensional retina and choroid angiography. *J Biomed Opt*. 2010; 15:016029.
77. Fingler J, Zawadzki RJ, Werner JS, Schwartz D, Fraser SE. Volumetric microvascular imaging of human retina using optical coherence tomography with a novel motion contrast technique. *Opt Express*. 2009;17:22190–22200.
78. Mwanza JC, Budenz DL. Optical coherence tomography platforms and parameters for glaucoma diagnosis and progression. *Curr Opin Ophthalmol*. 2015.
79. Strouthidis NG, Scott A, Peter NM, Garway-Heath DF. Optic disc and visual field progression in ocular hypertensive subjects: detection rates, specificity, and agreement. *Invest Ophthalmol Vis Sci*. 2006;47:2904–2910.
80. Medeiros FA, Alencar LM, Zangwill LM, Bowd C, Sample PA, Weinreb RN. Prediction of functional loss in glaucoma from progressive optic disc damage. *Arch Ophthalmol*. 2009;127: 1250–1256.
81. Artes PH, Chauhan BC. Longitudinal changes in the visual field and optic disc in glaucoma. *Prog Retin Eye Res*. 2005; 24:333–354.
82. Quigley HA, Katz J, Derick RJ, Gilbert D, Sommer A. An evaluation of optic disc and nerve fiber layer examinations in monitoring progression of early glaucoma damage. *Ophthalmology*. 1992;99:19–28.
83. Sommer A, Katz J, Quigley HA, et al. Clinically detectable nerve fiber atrophy precedes the onset of glaucomatous field loss. *Arch Ophthalmol*. 1991;109:77–83.
84. Kuang TM, Zhang C, Zangwill LM, Weinreb RN, Medeiros FA. Estimating lead time gained by optical coherence tomography in detecting glaucoma before development of visual field defects. *Ophthalmology*. 2015;122:2002–2009.
85. Katz J, Quigley HA, Sommer A. Repeatability of the Glaucoma Hemifield Test in automated perimetry. *Invest Ophthalmol Vis Sci*. 1995;36:1658–1664.
86. Spry PG, Johnson CA, McKendrick AM, Turpin A. Measurement error of visual field tests in glaucoma. *Br J Ophthalmol*. 2003;87:107–112.
87. Ederer F, Gaasterland DE, Sullivan EK, Investigators A. The Advanced Glaucoma Intervention Study (AGIS): 1. Study design and methods and baseline characteristics of study patients. *Control Clin Trials*. 1994;15:299–325.
88. Leske MC, Heijl A, Hyman L, Bengtsson B. Early manifest glaucoma trial: design and baseline data. *Ophthalmology*. 1999;106:2144–2153.
89. Musch DC, Lichter PR, Guire KE, Standardi CL. The Collaborative Initial Glaucoma Treatment Study: study design, methods, and baseline characteristics of enrolled patients. *Ophthalmology*. 1999;106:653–662.
90. Gracitelli CP, Abe RY, Medeiros FA. Spectral-domain optical coherence tomography for glaucoma diagnosis. *Open Ophthalmol J*. 2015;9:68–77.
91. Pederson JE, Anderson DR. The mode of progressive disc cupping in ocular hypertension and glaucoma. *Arch Ophthalmol*. 1980;98:490–495.
92. Jonas JB, Fernandez MC, Sturmer J. Pattern of glaucomatous neuroretinal rim loss. *Ophthalmology*. 1993;100:63–68.
93. Airaksinen PJ, Tuulonen A, Alanko HI. Rate and pattern of neuroretinal rim area decrease in ocular hypertension and glaucoma. *Arch Ophthalmol*. 1992;110:206–210.
94. Yang Z, Tatham AJ, Zangwill LM, Weinreb RN, Zhang C, Medeiros FA. Diagnostic ability of retinal nerve fiber layer imaging by swept-source optical coherence tomography in glaucoma. *Am J Ophthalmol*. 2015;159:193–201.
95. Leite MT, Zangwill LM, Weinreb RN, et al. Effect of disease severity on the performance of Cirrus spectral-domain OCT for glaucoma diagnosis. *Invest Ophthalmol Vis Sci*. 2010;51: 4104–4019.
96. Bengtsson B, Andersson S, Heijl A. Performance of time-domain and spectral-domain optical coherence tomography for glaucoma screening. *Acta Ophthalmol*. 2012;90:310–315.

Investigative Ophthalmology & Visual Science

97. Mwanza JC, Chang RT, Budenz DL, et al. Reproducibility of peripapillary retinal nerve fiber layer thickness and optic nerve head parameters measured with cirrus HD-OCT in glaucomatous eyes. *Invest Ophthalmol Vis Sci*. 2010;51:5724–5730.
98. Traynis I, De Moraes CG, Raza AS, Liebmann JM, Ritch R, Hood DC. Prevalence and nature of early glaucomatous defects in the central 10 degrees of the visual field. *JAMA Ophthalmol*. 2014;132:291–297.
99. Hood DC, Slobodnick A, Raza AS, de Moraes CG, Teng CC, Ritch R. Early glaucoma involves both deep local, and shallow widespread, retinal nerve fiber damage of the macular region. *Invest Ophthalmol Vis Sci*. 2014;55:632–649.
100. Hood DC, Raza AS, de Moraes CG, Liebmann JM, Ritch R. Glaucomatous damage of the macula. *Prog Retin Eye Res*. 2013;32:1–21.
101. Hood DC, Raza AS, de Moraes CG, Odel JG, Greenstein VC, Liebmann JM, et al. Initial arcuate defects within the central 10 degrees in glaucoma. *Invest Ophthalmol Vis Sci*. 2011;52:940–946.
102. Schiefer U, Papageorgiou E, Sample PA, et al. Spatial pattern of glaucomatous visual field loss obtained with regionally condensed stimulus arrangements. *Invest Ophthalmol Vis Sci*. 2010;51:5685–5689.
103. Anctil JL, Anderson DR. Early foveal involvement and generalized depression of the visual field in glaucoma. *Arch Ophthalmol*. 1984;102:363–370.
104. Nicholas SP, Werner EB. Location of early glaucomatous visual field defects. *Can J Ophthalmol*. 1980;15:131–133.
105. Henson DB, Hobley AJ. Frequency distribution of early glaucomatous visual field defects. *Am J Optom Physiol Opt*. 1986;63:455–461.
106. Wang DL, Raza AS, de Moraes CG, et al. Central glaucomatous damage of the macula can be overlooked by conventional OCT retinal nerve fiber layer thickness analyses. *Trans Vis Sci Tech*. 2015;4(6):4.
107. Heijl A, Lundqvist L. The frequency distribution of earliest glaucomatous visual field defects documented by automatic perimetry. *Acta Ophthalmol (Copenh)*. 1984;62:658–664.
108. Keltner JL, Johnson CA, Cello KE, et al. Classification of visual field abnormalities in the ocular hypertension treatment study. *Arch Ophthalmol*. 2003;121:643–650.
109. Arintawati P, Sone T, Akita T, Tanaka J, Kiuchi Y. The applicability of ganglion cell complex parameters determined from SD-OCT images to detect glaucomatous eyes. *J Glaucoma*. 2013;22:713–718.
110. Sung KR, Wollstein G, Kim NR, et al. Macular assessment using optical coherence tomography for glaucoma diagnosis. *Br J Ophthalmol*. 2012;96:1452–1455.
111. Tan O, Li G, Lu AT, Varma R, Huang D. Advanced Imaging for Glaucoma Study Group. Mapping of macular substructures with optical coherence tomography for glaucoma diagnosis. *Ophthalmology*. 2008;115:949–956.
112. Inuzuka H, Kawase K, Sawada A, Kokuzawa S, Ishida K, Yamamoto T. Development of glaucomatous visual field defects in preperimetric glaucoma patients within 3 years of diagnosis. *J Glaucoma*. 2016;25:e591–e595.
113. Curcio CA, Allen KA. Topography of ganglion cells in human retina. *J Comp Neurol*. 1990;300:5–25.
114. Jeong JS, Kang MG, Kim CY, Kim NR. Pattern of macular ganglion cell-inner plexiform layer defect generated by spectral-domain OCT in glaucoma patients and normal subjects. *J Glaucoma*. 2015;24:583–590.
115. Mwanza JC, Oakley JD, Budenz DL, Chang RT, Knight OJ, Feuer WJ. Macular ganglion cell-inner plexiform layer: automated detection and thickness reproducibility with spectral domain-optical coherence tomography in glaucoma. *Invest Ophthalmol Vis Sci*. 2011;52:8323–8329.
116. Syc SB, Saidha S, Newsome SD, et al. Optical coherence tomography segmentation reveals ganglion cell layer pathology after optic neuritis. *Brain*. 2012;135:521–533.
117. Mwanza JC, Durbin MK, Budenz DL, et al. Glaucoma diagnostic accuracy of ganglion cell-inner plexiform layer thickness: comparison with nerve fiber layer and optic nerve head. *Ophthalmology*. 2012;119:1151–1158.
118. Kotowski J, Folio LS, Wollstein G, et al. Glaucoma discrimination of segmented cirrus spectral domain optical coherence tomography (SD-OCT) macular scans. *Br J Ophthalmol*. 2012;96:1420–1425.
119. Lee KM, Lee EJ, Kim TW, Kim H. Comparison of the Abilities of SD-OCT and SS-OCT in evaluating the thickness of the macular inner retinal layer for glaucoma diagnosis. *PLoS One*. 2016;11:e0147964.
120. Martinez-de-la-Casa JM, Cifuentes-Canorea P, Berrozpe C, et al. Diagnostic ability of macular nerve fiber layer thickness using new segmentation software in glaucoma suspects. *Invest Ophthalmol Vis Sci*. 2014;55:8343–8348.
121. Tan O, Chopra V, Lu AT, et al. Detection of macular ganglion cell loss in glaucoma by Fourier-domain optical coherence tomography. *Ophthalmology*. 2009;116:2305–2314.
122. Lisboa R, Paranhos A, Jr., Weinreb RN, Zangwill LM, Leite MT, Medeiros FA. Comparison of different spectral domain OCT scanning protocols for diagnosing preperimetric glaucoma. *Invest Ophthalmol Vis Sci*. 2013;54:3417–3425.
123. Na JH, Sung KR, Baek S, Sun JH, Lee Y. Macular and retinal nerve fiber layer thickness: which is more helpful in the diagnosis of glaucoma? *Invest Ophthalmol Vis Sci*. 2011;52:8094–8101.
124. Kim NR, Lee ES, Seong GJ, Kim JH, An HG, Kim CY. Structure-function relationship and diagnostic value of macular ganglion cell complex measurement using Fourier-domain OCT in glaucoma. *Invest Ophthalmol Vis Sci*. 2010;51:4646–4651.
125. Mansouri K, Leite MT, Medeiros FA, Leung CK, Weinreb RN. Assessment of rates of structural change in glaucoma using imaging technologies. *Eye (Lond)*. 2011;25:269–277.
126. Zangalli CS, Ahmed OM, Waisbourd M, et al. Segmental analysis of macular layers in patients with unilateral primary open-angle glaucoma. *J Glaucoma*. 2015;25:e401–e407.
127. Seong M, Sung KR, Choi EH, et al. Macular and peripapillary retinal nerve fiber layer measurements by spectral domain optical coherence tomography in normal-tension glaucoma. *Invest Ophthalmol Vis Sci*. 2010;51:1446–1452.
128. Schulze A, Lamparter J, Pfeiffer N, Berisha F, Schmidtmann I, Hoffmann EM. Diagnostic ability of retinal ganglion cell complex, retinal nerve fiber layer, and optic nerve head measurements by Fourier-domain optical coherence tomography. *Graefes Arch Clin Exp Ophthalmol*. 2011;249:1039–1045.
129. Garas A, Vargha P, Hollo G. Diagnostic accuracy of nerve fibre layer, macular thickness and optic disc measurements made with the RTVue-100 optical coherence tomograph to detect glaucoma. *Eye (Lond)*. 2011;25:57–65.
130. Yang Z, Tatham AJ, Weinreb RN, Medeiros FA, Liu T, Zangwill LM. Diagnostic ability of macular ganglion cell inner plexiform layer measurements in glaucoma using swept source and spectral domain optical coherence tomography. *PLoS One*. 2015;10:e0125957.
131. Hood DC, Raza AS, de Moraes CG, Johnson CA, Liebmann JM, Ritch R. The nature of macular damage in glaucoma as revealed by averaging optical coherence tomography data. *Trans Vis Sci Tech*. 2012;1:3.
132. Kotera Y, Hangai M, Hirose F, Mori S, Yoshimura N. Three-dimensional imaging of macular inner structures in glaucoma by using spectral-domain optical coherence tomography. *Invest Ophthalmol Vis Sci*. 2011;52:1412–1421.

Investigative Ophthalmology & Visual Science

133. Hollo G, Shu-Wei H, Naghizadeh F. Evaluation of a new software version of the RTVue optical coherence tomograph for image segmentation and detection of glaucoma in high myopia. *J Glaucoma*. 2015;25:e615–e619.
134. Hollo G, Naghizadeh F. Influence of a new software version of the RTVue-100 optical coherence tomograph on the detection of glaucomatous structural progression. *Eur J Ophthalmol*. 2015;25:410–415.
135. Asrani S, Rosdahl JA, Allingham RR. Novel software strategy for glaucoma diagnosis: asymmetry analysis of retinal thickness. *Arch Ophthalmol*. 2011;129:1205–1211.
136. Kochendorfer L, Bauer P, Funk J, Toteberg-Harms M. Posterior pole asymmetry analysis with optical coherence tomography. *Klin Monbl Augenheilkd*. 2014;231:368–373.
137. Dave P, Shah J. Diagnostic accuracy of posterior pole asymmetry analysis parameters of spectralis optical coherence tomography in detecting early unilateral glaucoma. *Indian J Ophthalmol*. 2015;63:837–842.
138. Seo JH, Kim TW, Weinreb RN, Park KH, Kim SH, Kim DM. Detection of localized retinal nerve fiber layer defects with posterior pole asymmetry analysis of spectral domain optical coherence tomography. *Invest Ophthalmol Vis Sci*. 2012;53:4347–4353.
139. Zhang X, Loewen N, Tan O, et al. Predicting development of glaucomatous visual field conversion using baseline Fourier-domain optical coherence tomography. *Am J Ophthalmol*. 2015;163:29–37.
140. Jaffe GJ, Caprioli J. Optical coherence tomography to detect and manage retinal disease and glaucoma. *Am J Ophthalmol*. 2004;137:156–169.
141. Kasumovic SS, Pavljasevic S, Cabric E, Mavija M, Dacic-Lepara S, Jankov M. Correlation between retinal nerve fiber layer and disc parameters in glaucoma suspected eyes. *Med Arch*. 2014;68:113–116.
142. Pollet-Villard F, Chiquet C, Romanet JP, Noel C, Aptel F. Structure-function relationships with spectral-domain optical coherence tomography retinal nerve fiber layer and optic nerve head measurements. *Invest Ophthalmol Vis Sci*. 2014;55:2953–2962.
143. Sung KR, Na JH, Lee Y. Glaucoma diagnostic capabilities of optic nerve head parameters as determined by Cirrus HD optical coherence tomography. *J Glaucoma*. 2012;21:498–504.
144. Sugimoto M, Ito K, Goto R, Uji Y. Symmetry analysis for detecting early glaucomatous changes in ocular hypertension using optical coherence tomography. *Jpn J Ophthalmol*. 2004;48:281–286.
145. Medeiros FA. How should diagnostic tests be evaluated in glaucoma? *Br J Ophthalmol*. 2007;91:273–274.
146. Wong EY, Keeffe JE, Rait JL, et al. Detection of undiagnosed glaucoma by eye health professionals. *Ophthalmology*. 2004;111:1508–1514.
147. Kong YX, Coote MA, O'Neill EC, et al. Glaucomatous optic neuropathy evaluation project: a standardized internet system for assessing skills in optic disc examination. *Clin Experiment Ophthalmol*. 2011;39:308–317.
148. Chauhan BC, O'Leary N, Almobarak FA, et al. Enhanced detection of open-angle glaucoma with an anatomically accurate optical coherence tomography-derived neuroretinal rim parameter. *Ophthalmology*. 2013;120:535–543.
149. Reis AS, O'Leary N, Yang H, et al. Influence of clinically invisible, but optical coherence tomography detected, optic disc margin anatomy on neuroretinal rim evaluation. *Invest Ophthalmol Vis Sci*. 2012;53:1852–1860.
150. Chauhan BC, Burgoyne CF. From clinical examination of the optic disc to clinical assessment of the optic nerve head: a paradigm change. *Am J Ophthalmol*. 2013;156:218–227.
151. Danthurebandara VM, Sharpe GP, Hutchison DM, et al. Enhanced structure-function relationship in glaucoma with an anatomically and geometrically accurate neuroretinal rim measurement. *Invest Ophthalmol Vis Sci*. 2015;56:98–105.
152. Banegas SA, Anton A, Morilla A, et al. Evaluation of the retinal nerve fiber layer thickness, the mean deviation, and the visual field index in progressive glaucoma. *J Glaucoma*. 2015;25:e229–e235.
153. Wessel JM, Horn FK, Tornow RP, et al. Longitudinal analysis of progression in glaucoma using spectral-domain optical coherence tomography. *Invest Ophthalmol Vis Sci*. 2013;54:3613–3620.
154. Na JH, Sung KR, Lee JR, et al. Detection of glaucomatous progression by spectral-domain optical coherence tomography. *Ophthalmology*. 2013;120:1388–1395.
155. Na JH, Sung KR, Baek S, Lee JY, Kim S. Progression of retinal nerve fiber layer thinning in glaucoma assessed by cirrus optical coherence tomography-guided progression analysis. *Curr Eye Res*. 2013;38:386–395.
156. Leung CK, Cheung CY, Weinreb RN, et al. Evaluation of retinal nerve fiber layer progression in glaucoma: a study on optical coherence tomography guided progression analysis. *Invest Ophthalmol Vis Sci*. 2010;51:217–222.
157. Wollstein G, Kagemann L, Bilonick RA, et al. Retinal nerve fibre layer and visual function loss in glaucoma: the tipping point. *Br J Ophthalmol*. 2012;96:47–52.
158. Vazirani J, Kaushik S, Pandav SS, Gupta P. Reproducibility of retinal nerve fiber layer measurements across the glaucoma spectrum using optical coherence tomography. *Indian J Ophthalmol*. 2015;63:300–305.
159. Shon K, Wollstein G, Schuman JS, Sung KR. Prediction of glaucomatous visual field progression: pointwise analysis. *Curr Eye Res*. 2014;39:705–710.
160. Sehi M, Zhang X, Greenfield DS, et al. Retinal nerve fiber layer atrophy is associated with visual field loss over time in glaucoma suspect and glaucomatous eyes. *Am J Ophthalmol*. 2013;155:73–82.
161. Sung KR, Sun JH, Na JH, Lee JY, Lee Y. Progression detection capability of macular thickness in advanced glaucomatous eyes. *Ophthalmology*. 2012;119:308–313.
162. Na JH, Sung KR, Baek S, et al. Detection of glaucoma progression by assessment of segmented macular thickness data obtained using spectral domain optical coherence tomography. *Invest Ophthalmol Vis Sci*. 2012;53:3817–3826.
163. Medeiros FA, Zangwill LM, Girkin CA, Liebmann JM, Weinreb RN. Combining structural and functional measurements to improve estimates of rates of glaucomatous progression. *Am J Ophthalmol*. 2012;153:1197–1205.
164. Medeiros FA, Leite MT, Zangwill LM, Weinreb RN. Combining structural and functional measurements to improve detection of glaucoma progression using Bayesian hierarchical models. *Invest Ophthalmol Vis Sci*. 2011;52:5794–5803.
165. Tatham AJ, Weinreb RN, Medeiros FA. Strategies for improving early detection of glaucoma: the combined structure-function index. *Clin Ophthalmol*. 2014;8:611–621.
166. Belghith A, Bowd C, Medeiros FA, Balasubramanian M, Weinreb RN, Zangwill LM. Learning from healthy and stable eyes: a new approach for detection of glaucomatous progression. *Artif Intell Med*. 2015;64:105–115.
167. El Beltagi TA, Bowd C, Boden C, et al. Retinal nerve fiber layer thickness measured with optical coherence tomography is related to visual function in glaucomatous eyes. *Ophthalmology*. 2003;110:2185–2191.
168. Lan YW, Henson DB, Kwartz AJ. The correlation between optic nerve head topographic measurements, peripapillary nerve fibre layer thickness, and visual field indices in glaucoma. *Br J Ophthalmol*. 2003;87:1135–1141.

169. Weinreb RN, Shakiba S, Sample PA, et al. Association between quantitative nerve fiber layer measurement and visual field loss in glaucoma. *Am J Ophthalmol*. 1995;120:732–738.
170. Hoffmann EM, Medeiros FA, Sample PA, et al. Relationship between patterns of visual field loss and retinal nerve fiber layer thickness measurements. *Am J Ophthalmol*. 2006;141: 463–471.
171. Horn FK, Mardin CY, Laemmer R, et al. Correlation between local glaucomatous visual field defects and loss of nerve fiber layer thickness measured with polarimetry and spectral domain OCT. *Invest Ophthalmol Vis Sci*. 2009;50:1971–1977.
172. Kanamori A, Naka M, Nagai-Kusuhara A, Yamada Y, Nakamura M, Negi A. Regional relationship between retinal nerve fiber layer thickness and corresponding visual field sensitivity in glaucomatous eyes. *Arch Ophthalmol*. 2008;126:1500–1506.
173. Grewal DS, Sehi M, Paauw JD, Greenfield DS. Advanced Imaging in Glaucoma Study Group. Detection of progressive retinal nerve fiber layer thickness loss with optical coherence tomography using 4 criteria for functional progression. *J Glaucoma*. 2012;21:214–220.
174. Varma R, Quigley HA, Pease ME. Changes in optic disk characteristics and number of nerve fibers in experimental glaucoma. *Am J Ophthalmol*. 1992;114:554–559.
175. Grytz R, Meschke G, Jonas JB. The collagen fibril architecture in the lamina cribrosa and peripapillary sclera predicted by a computational remodeling approach. *Biomech Model Mechanobiol*. 2011;10:371–382.
176. Wang B, Nevins JE, Nadler Z, et al. Reproducibility of in-vivo OCT measured three-dimensional human lamina cribrosa microarchitecture. *PLoS One*. 2014;9:e95526.
177. Wang B, Nevins JE, Nadler Z, et al. In vivo lamina cribrosa micro-architecture in healthy and glaucomatous eyes as assessed by optical coherence tomography. *Invest Ophthalmol Vis Sci*. 2013;54:8270–8274.
178. Miller KM, Quigley HA. Comparison of optic disc features in low-tension and typical open-angle glaucoma. *Ophthalmic Surg*. 1987;18:882–889.
179. Tezel G, Trinkaus K, Wax MB. Alterations in the morphology of lamina cribrosa pores in glaucomatous eyes. *Br J Ophthalmol*. 2004;88:251–256.
180. Jung KI, Jeon S, Park CK. Lamina cribrosa depth is associated with the cup-to-disc ratio in eyes with large optic disc cupping and cup-to-disc ratio asymmetry. *J Glaucoma*. 2016; 25:e536–e545.
181. Sawada Y, Hangai M, Murata K, Ishikawa M, Yoshitomi T. Lamina cribrosa depth variation measured by spectral-domain optical coherence tomography within and between four glaucomatous optic disc phenotypes. *Invest Ophthalmol Vis Sci*. 2015;56:5777–5784.
182. Kim YW, Kim DW, Jeoung JW, Kim DM, Park KH. Peripheral lamina cribrosa depth in primary open-angle glaucoma: a swept-source optical coherence tomography study of lamina cribrosa. *Eye (Lond)*. 2015;29:1368–1374.
183. Chung HS, Sung KR, Lee JY, Na JH. Lamina cribrosa-related parameters assessed by optical coherence tomography for prediction of future glaucoma progression. *Curr Eye Res*. 2016;41:806–813.
184. Morgan-Davies J, Taylor N, Hill AR, Aspinall P, O'Brien CJ, Azuara-Blanco A. Three dimensional analysis of the lamina cribrosa in glaucoma. *Br J Ophthalmol*. 2004;88:1299–1304.
185. Quigley HA. Glaucoma. *Lancet*. 2011;377:1367–1377.
186. Burgoyne CF. A biomechanical paradigm for axonal insult within the optic nerve head in aging and glaucoma. *Exp Eye Res*. 2011;93:120–132.
187. Gotzinger E, Pircher M, Baumann B, Hirn C, Vass C, Hitzenberger CK. Retinal nerve fiber layer birefringence evaluated with polarization sensitive spectral domain OCT and scanning laser polarimetry: a comparison. *J Biophotonics*. 2008;1:129–139.
188. Cense B, Koperda E, Brown JM, et al. Volumetric retinal imaging with ultrahigh-resolution spectral-domain optical coherence tomography and adaptive optics using two broadband light sources. *Opt Express*. 2009;17:4095–4111.
189. Srinivasan VJ, Adler DC, Chen Y, et al. Ultrahigh-speed optical coherence tomography for three-dimensional and en face imaging of the retina and optic nerve head. *Invest Ophthalmol Vis Sci*. 2008;49:5103–5110.

Investigative Ophthalmology & Visual Science